

# Determination of the Most Accurate Horizontal to Tilted Sky-Diffuse Solar Irradiation Transposition Model for the Capital Cities in MENA Region

Yasser F. Nassar

Mechanical and Industrial  
Eng. Dept.  
Faculty of Eng. & Tech. Sebha  
Universit, Brack, Libya  
[yas.nassar1@sebhau.edu.ly](mailto:yas.nassar1@sebhau.edu.ly)

Samer Y. Alsadi

Electrical Eng. Dept.  
Palestine Technical Univ.-  
Kadoorie  
Tulkarm-Palestine  
[s.alsadi@ptuk.edu.ps](mailto:s.alsadi@ptuk.edu.ps)

Hala J. El-Khozondar

Electrical Engineering and  
smart systems Dept., Islamic  
University of Gaza, Gaza,  
Palestine  
[hkhonzondar@iugaza.edu.ps](mailto:hkhonzondar@iugaza.edu.ps)

Shady S. Refaat

Dept. of Elect. and computer  
Engineering  
Texas A&M at Qatar  
Doha, Qatar  
[shady.khalil@qatar.tamu.edu](mailto:shady.khalil@qatar.tamu.edu)

**Abstract** - Accurate solar radiation data is essential in designing, evaluating and optimizing solar energy systems. The meteorological recorded data is the mainly source of the solar irradiance data. Since solar irradiance incident on a specific tilted surface is not frequently recorded, the horizontal to tilted solar irradiation transposition models (HTTM) use to convert the measurable components of solar irradiation (global horizontal, sky-diffuse and ground reflected) to global tilted solar irradiation with high accuracy. The importance of the solar transposition model is in determining the optimum tilt angle of solar energy harvesters which is one of the important design parameters for maximizing solar radiation incident on the solar collectors. This paper introduces a statistical procedure to figure out the transposition model that is closest to the real model in the MENA region without needs for measured data. Also it provided a summary of optimum tilt angles and transposition models that recommended by local researchers for specific locations in MENA region. This study showed that the transposition models depend on the angle of inclination of the solar collector in addition to the location. The study identified models with deviation rates about 3% for most cities, which is an engineering reasonable percentage, and this encourages the authors to recommend this approach to determine more accurate transposition models for wider regions of the world. On the other hand, it showed that all models failed to achieve an acceptable deviation rate for high tilt angles especially vertical surfaces, which have great engineering applications. The authors advise researchers to take care when adopting a transposition model that has been validated at low tilt angles to apply it to high tilt angles and building façades. The study is also reveal that, the reduction in total annual global solar irradiation is not exceed than 1% due to the offset of tilt angle from the optimum angle for all considered transposition models and for all sites.

**Index Terms** - Optimum tilt angle, transposition model, solar energy, MENA, solar irradiance

## I. INTRODUCTION

The intensity of solar irradiance incident on the earth surface fluctuates as a result of continually changing of the sun position in the sky dome. This angular movement is prescribed in all textbooks of solar energy, as a function of  $(n, h)$  where  $n$  is the Julian day and  $h$  is the time [1, 2]. To maintain the highest level of solar radiation, the surface must be tilted at a certain angle, such that it can capture maximum solar energy. This approach can be instantaneous, as is the case of solar tracking systems [3], daily, monthly, seasonal, or fixed on one angle throughout the year [4]. Many studies have been conducted to obtain the annual optimal tilt angle ( $\beta_{opt}$ ) for different locations as a function of latitude [4-6], weather data [7], and character of the energy demand [8-10].

The accurate determination of  $\beta_{opt}$  for any location is essential for maximum energy production by the system [11]. Hafez et al. reviewed the recommended optimum tilt angles with respect to solar altitude and latitude angles for several solar energy applications [12]. Many researchers have calculated the optimum tilt angles for many locations in MENA region, for example but not limited to: Assuit-Egypt [13], Najaf-Iraq [14], Kano-Nigeria [15], Settat-Morocco [16], Tabass-Iran [17], Gaza-Palestine [18]. Other researches attempt to derive a general expression for large zone, such as: Saudi [19], Algeria [20], Palestine [21], Turkey [22], Egypt [23], Iran [24], Arabic countries [4], Mediterranean Region [6], desert regions [25], high latitudes [26], northern hemisphere [27], all the world [28].

The theoretical approach for obtaining the optimum tilt angle of a solar collector at any location is passed through three steps: First, obtaining the horizontal solar irradiation components, which are: the beam normal ( $I_{bn}$ ) and the sky diffuse irradiance ( $I_{dn}$ ). Second, identifying the appropriate HTTM in order to convert the horizontal solar irradiance to tilted solar irradiance. Finally, getting the maximum solar irradiance during an interval of time and the corresponding tilt angle value by simulating the tilted solar irradiance over large range of tilt angles ( $0^\circ \leq \beta \leq 90^\circ$ ). The certainty of the results is highly relying upon the accuracy of the solar irradiance components and the precision of the HTTM. These two requirements are very particularity for each specific location, and must be identified in advance before starting the optimization process. However, knowledge of the appropriate HTTM needs for measurements of the solar irradiation components at different tilt and azimuth angles for each location. Which in most cases is not available, and if it does exist, then the information is insufficient to figure out the correct HTTM. Although many studies opposed the use of isotropic models, nevertheless Tables 1 and 2 strongly demonstrate the availability of Liu & Jordan model to represent solar radiation data and still used to determine the optimum tilt angle in many scientific works [29-33].

This study comes to clarify the role of HTTM on the accuracy of the calculations in terms of the intensity of solar radiation and the optimum tilt angle.

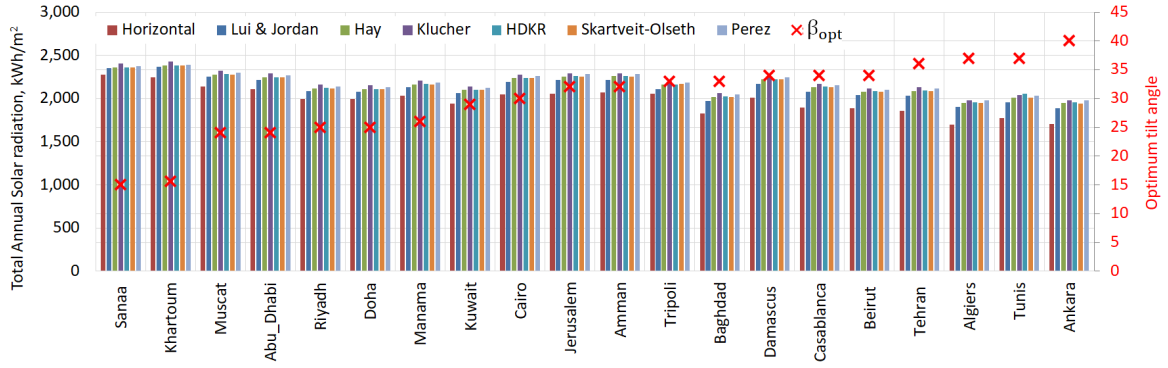


Fig.1: The optimum tilt angle and the corresponding total annual global tilted solar radiation [kWh/m<sup>2</sup>] by several HTTM for Capital cities of countries in MENA region

## II. METHODOLOGY

The approach begins with collecting the horizontal solar irradiation components for a certain location, and then the data will be processed by applying the most widely used HTTM (Liu&Jordan, HDKR, Klucher, Hey, Skartveit&Olseth, and Perez) via the MS Excel. As a result of the analysis, it can be locate the most accurate model for each location.

### A. Calculation of global tilted solar irradiance

The global horizontal solar irradiance ( $I_h$ ) consists of direct beam ( $I_{bh}$ ) and sky-diffuse ( $I_{dh}$ ) components, and estimated directly from the following relations [1]:

$$I_h = I_{bh} + I_{dh}, \text{ So} \quad (1)$$

$$I_{bh} = I_h - I_{dh} \quad (2)$$

Table 1: Commercial software of solar systems and the corresponding transposition models that used

| No | Software           | Transposition model   |
|----|--------------------|---|
| 1  | NASA               | Liu & Jordan  |
| 2  | SOLARGIS           | Muneer  |
| 3  | Solcast            | Reindl  |
| 4  | Global solar atlas | Perez   |
| 5  | SoDa               | Muneer  |
|    | Meteonorm          | Hay, Skartveit & Olseth   |
| 6  | Meteoblue AG       | HDKR  |
| 7  | EnergyPro          | HDKR  |
| 8  | HOMER              | HDKR  |
| 9  | INSEL              | Liu & Jordan, Temps & Coulson, Bugler, Klucher, Hay, Willmott, Skartveit & Olseth, Gueymard, Perez and HDKR |
| 10 | PVToolbox          | Liu & Jordan  |
| 11 | Polysun            | Hay & Davies  |
| 12 | PV F-chart         | Liu & Jordan  |
| 13 | PV*Sol             | Skartveit & Olseth, HDKR and Perez  |
| 14 | PVDesign           | HDKR and Perez  |
| 15 | PVForm             | Perez   |
| 16 | PVGIS              | Muneer  |
| 17 | PVplanner          | Perez   |
| 18 | PVSyst             | Hay and Perez   |
| 19 | PVWatts            | Perez   |
| 20 | RAPSIM             | Unknown   |
| 21 | RETscreen          | Liu & Jordan  |
| 22 | SAM                | Liu & Jordan, Hay & Davies, Perez and HDKR  |
| 23 | SimulationX        | Liu & Jordan  |
| 24 | Solar Pro          | Unknown   |
| 25 | SolarSizer         | Unknown   |
| 26 | TRNSYS             | HDKR  |

Estimation of solar irradiance on tilted planes ( $I_t$ ) can be performed as [1]:

$$I_t = I_{bt} + I_{dt} + I_{rt} \quad (3)$$

Where  $I_{bt}$ ,  $I_{dt}$  and  $I_{rt}$  are the tilted plane beam, diffuse and ground reflected solar irradiances.

Eq. (3) can be rewritten again in terms of the available data ( $I_{bh}$  and  $I_{dh}$ ) as following [1]:

$$I_t = I_{bh}R_b + I_{dh}R_d + I_h R_r \quad (4)$$

The conversion of direct radiation is straight forward and it is common to use the transportation factor  $R_b$  which is a function of geometrical parameters of the inclined surface and the position of the sun, which equal to [1]:

$$R_b = \max\left(0, \frac{\cos \theta_i}{\cos \theta_z}\right) \quad (5)$$

Where:  $\theta_i$ ,  $\theta_z$  are the solar incidence and zenith angles, respectively.  $R_d$  and  $R_r$  are the sky and the ground transposition factors, respectively. Over the years, many authors have presented albedo transposition models. While it is common to assume isotropic albedo radiation [1]:

$$R_r = \rho_g \frac{1 - \cos \beta}{2} \quad (6)$$

Where  $\beta$  is the surface tilt angle,  $\rho_g$  refers to the ground reflectivity or albedo and it considered as 0.2 in most cases [34].

The diffuse irradiance is calculated by using several models [35]:

#### 1. Liu & Jordan model; 1963 (L):

$$R_d = \frac{(1 + \cos \beta)}{2} \quad (7)$$

#### 2. Klucher model; 1979 (K):

$$R_d = \left(\cos^2 \frac{\beta}{2}\right) \left(1 + f_k \cos^2 \theta_i \sin^3 \theta_z\right) \left(1 + f_k \sin^3 \left(\frac{\beta}{2}\right)\right), f_k = 1 - \left(\frac{I_{dh}}{I_h}\right)^2 \quad (8)$$

#### 3. Skartveit-Olseth model; 1986 (S):

$$R_d = F_{Hay}R_b + Z \cos \beta + (1 - F_{Hay} - Z) \cos^2 \left(\frac{\beta}{2}\right), Z = \max[(0.3 - 2F_{Hay}), 0] \quad (9)$$

#### Perez model; 1990 (P):

$$R_d = F_1 \frac{a}{b} + (1 - F_1) \left(\frac{1 + \cos \beta}{2}\right) + F_2 \sin \beta \quad (10)$$

$$a = \max(0, \cos \theta_i)$$

$$b = \max(\cos 85^\circ, \sin \gamma)$$

$$F_1 = F_{11}(\varepsilon) + F_{12}(\varepsilon)\Delta + F_{13}(\varepsilon)\theta_z$$

$$F_2 = F_{21}(\varepsilon) + F_{22}(\varepsilon)\Delta + F_{23}(\varepsilon)\theta_z$$

$$\varepsilon = \frac{I_{dh} + 1.041\theta_z^3}{1 + 1.041\theta_z^3} \text{ and } \Delta = M \frac{I_{dh}}{I_{ext}}$$

Where  $\theta_z$  is in radians and  $M$  is the optical air mass, Perez has published many versions of the  $F_{ij}$  coefficients for many locations. Table 3 tabulate the  $F_{ij}$  coefficients for 1990 Perez's model.

Table 3: Perez sky irradiance model coefficients (1990)

| $\varepsilon$ | $F_{11}$ | $F_{12}$ | $F_{13}$ | $F_{21}$ | $F_{22}$ | $F_{23}$ |
|---------------|----------|----------|----------|----------|----------|----------|
| 1.000-1.065   | -0.008   | 0.588    | -0.062   | -0.060   | 0.072    | -0.022   |
| 1.065-1.230   | 0.130    | 0.683    | -0.151   | -0.019   | 0.066    | -0.029   |
| 1.230-1.500   | 0.330    | 0.487    | -0.221   | 0.055    | -0.064   | -0.026   |
| 1.500-1.950   | 0.568    | 0.187    | -0.295   | 0.109    | -0.152   | 0.014    |
| 1.950-2.800   | 0.873    | -0.392   | -0.362   | 0.226    | -0.462   | 0.001    |
| 2.800-4.500   | 1.132    | -1.237   | -0.4112  | 0.288    | -0.823   | 0.056    |
| 4.500-6.200   | 1.060    | -1.600   | -0.359   | 0.264    | -1.127   | 0.131    |
| >6.200        | 0.678    | -0.3327  | -0.250   | 0.156    | -1.377   | 0.251    |

#### 4. Hay, Davies, Klucher and Reindl model; 1990 (R):

$$R_d = F_{Hay}R_b + \left(1 - F_{Hay}\right) \left(\frac{1 + \cos\beta}{2}\right) \left[1 + f \sin^3\left(\frac{\beta}{2}\right)\right], \quad f = \sqrt{I_{bh}/I_h} \quad (11)$$

#### 5. Hay model; 1993 (H):

$$R_d = \hat{F}_{Hay}R_b + \left(1 - \hat{F}_{Hay}\right) \cos^2\left(\frac{\beta}{2}\right), \quad (12)$$

$$\hat{F}_{Hay} = I_{bh}/I_{sc}$$

#### B. Calculation of deviation rate (DR)

The deviation rate of certain HTTM ( $DR_i$ ) is a critical parameter in this research, and it expressed as:

$$DR_i\% = \frac{I_{t,i} - I_{t,j}}{I_{t,i}} \times 100 \quad (13)$$

$$i = 1, 2, \dots, n, \quad j = 1, 2, \dots, n \text{ and } i \neq j$$

Where  $I_{t,i}$  is the tilted solar irradiation calculated by using the transposition model ( $i$ ). So, for the considered six models the numbers of deviation rates for each transposition model are 5 values and then the largest value will be chosen.

### III. RESULTS AND DISCUSSION

Table 2: The optimum tilt angles recommended by several sources and the HTTM for the capital cities in MENA region

| Country   | City      | Lat.    | Long.   | Global solar atlas | PVGIS | NASA | PVWatts | SODA | Recommended HTTM |
|-----------|-----------|---------|---------|--------------------|-------|------|---------|------|------------------|
| Yemen     | Sanaa     | 15°21'N | 44°12'E | 20                 | 18    | 16   | 15      | 19   | N/A              |
| Sudan     | Khartoum  | 15°47'N | 32°43'E | 20                 | 18    | 16   | 15      | 19   | N/A              |
| Oman      | Muscat    | 23°35'N | 58°24'E | 24                 | 25    | 22   | 25      | 23   | Liu&Jordan [36]  |
| UAE       | Abu Dhabi | 24°28'N | 54°22'E | 24                 | 25    | 22   | 25      | 23   | N/A              |
| Saudi     | Riyadh    | 24°39'N | 46°46'E | 26                 | 25    | 23   | 24      | 23   | HDKR [29]        |
| Qatar     | Doha      | 25°18'N | 51°31'E | 25                 | 25    | 23   | 25      | 22   | N/A              |
| Bahrain   | Manama    | 26°13'N | 50°35'E | 24                 | 26    | 24   | 26      | 23   | N/A              |
| Kuwait    | Kuwait    | 29°22'N | 47°58'E | 27                 | 29    | 28   | 26      | 26   | N/A              |
| Egypt     | Cairo     | 30°2'N  | 31°13'E | 26                 | 28    | 28   | 25      | 27   | Klucher [37]     |
| Palestine | Jerusalem | 31°47'N | 35°13'E | 28                 | 28    | 29   | 26      | 27   | HDKR [35]        |
| Jordan    | Amman     | 31°57'N | 35°56'E | 29                 | 28    | 29   | 26      | 28   | N/A              |
| Libya     | Tripoli   | 32°52'N | 13°11'E | 29                 | 31    | 31   | 28      | 30   | N/A              |
| Iraq      | Baghdad   | 33°20'N | 44°23'E | 30                 | 31    | 31   | n/a     | 30   | Liu&Jordan [38]  |
| Syria     | Damascus  | 33°30'N | 36°18'E | 29                 | 29    | 31   | 29      | 29   | N/A              |

Due to the lack of solar radiation data for most locations of the study, these data were obtained free from the SoDa database [http://www.soda-pro.com/web-services/radiation/helioclim-3-archives-for-free], which are the global horizontal solar radiation ( $I_h$ ) and the component of the sky-diffuse solar irradiation ( $I_{dh}$ ). A MS Excel worksheet had been prepared to process the solar irradiation component in order to calculate the global tilted solar irradiation by using six HTTM, these are: Liu & Jordan, Hay, Klucher, Reindl, Skartvet&Olseth and Perez models corresponding to the optimum tilt angle of the solar collectors that recommended by local researches as it maintained in the introduction. The obtained results are graphically presented in Fig. 1 for all capital cities of the countries locate in MENA region.

Fig. 1 demonstrates the worth of determining the optimum tilt angle of solar collectors through the increase in irradiation from the horizontal surface, this augmentation in incident solar radiation is high as 16% for high latitude locations and reaches to 6% in low latitudes. Also, the total annual global solar radiation incident on an inclined surface at different tilt angles ( $10^\circ \leq \beta \leq 90^\circ$ ) was calculated for all the considered HTTMs. Then the percentage of deviation of each model from the rest of the models was calculated, and the largest value of deviation was chosen to represent the accuracy of that model. The aim of this step is to figure out the model with the least deviation, which represents the least risky model when used in case of absence of sufficient data to determine the correct model. Table 4 presents a colour scale of maximum deviation of each model from the rest of the models. Through the data included in the Table 4, it is possible to determine the least risky model (dark green color) for a specific location and at a specific angle of inclination. The results of the analysis indicate that both Liu&Jordan and Klucher models are the least accurate among the six selected models. The results also indicate a low accuracy rate for all the models considered when the angle of inclination is high ( $\beta > 60^\circ$ ) where the maximum deviation reaches to 11% at vertical surfaces. While models have been identified, the deviation rate is about 2% for most cities, which is a reasonable proportion geometrically, and this encourages the writers to use this method to determine more accurate relationships between wider regions of the world and test more models. Accordingly, it was able to recommend the most accuracy PHTM for each location and for each tilt angle as it tabulated in Table 5.

|         |            |         |         |    |    |    |     |    |                       |
|---------|------------|---------|---------|----|----|----|-----|----|-----------------------|
| Morocco | Casablanca | 33°32'N | 7°35'W  | 29 | 32 | 31 | 28  | 31 | Liu&Jordan [39]       |
| Lebanon | Beirut     | 33°54'N | 35°32'E | 28 | 29 | 30 | n/a | 29 | N/A                   |
| Iran    | Tehran     | 35°41'N | 51°25'E | 32 | 32 | 33 | 32  | 32 | Skartveit&Olseth [40] |
| Algeria | Algiers    | 36°42'N | 3°13'E  | 32 | 32 | 33 | 30  | 31 | Perez [41]            |
| Tunisia | Tunis      | 36°49'N | 10°11'E | 31 | 33 | 34 | 29  | 33 | N/A                   |
| Turkey  | Ankara     | 40°03'N | 32°52'E | 33 | 32 | 36 | 29  | 34 | N/A                   |

Table 4: Colour scale presentation of the Deviation rate of the HTTMs for all locations and under various tilt angles

|            | L                  | H | K | R | S | P | L                  | H | K | R | S | P |
|------------|--------------------|---|---|---|---|---|--------------------|---|---|---|---|---|
|            | $\beta = 10^\circ$ |   |   |   |   |   | $\beta = 20^\circ$ |   |   |   |   |   |
| Sanaa      | 4                  | 3 | 2 | 3 | 3 | 3 | 4                  | 3 | 3 | 3 | 3 | 2 |
| Khartoum   | 4                  | 3 | 3 | 3 | 3 | 3 | 4                  | 3 | 3 | 3 | 3 | 2 |
| Muscat     | 4                  | 3 | 3 | 3 | 3 | 3 | 4                  | 3 | 3 | 3 | 2 | 2 |
| Abu-Dhabi  | 4                  | 3 | 3 | 3 | 3 | 3 | 4                  | 3 | 3 | 3 | 3 | 2 |
| Riyadh     | 3                  | 3 | 3 | 3 | 3 | 2 | 3                  | 2 | 3 | 2 | 2 | 2 |
| Doha       | 4                  | 3 | 3 | 3 | 3 | 2 | 4                  | 2 | 3 | 2 | 2 | 2 |
| Manama     | 4                  | 3 | 3 | 3 | 3 | 2 | 4                  | 2 | 3 | 2 | 2 | 2 |
| Kuwait     | 4                  | 3 | 3 | 3 | 3 | 2 | 4                  | 2 | 3 | 2 | 2 | 2 |
| Cairo      | 4                  | 3 | 3 | 3 | 3 | 2 | 4                  | 2 | 3 | 2 | 2 | 2 |
| Jerusalem  | 4                  | 3 | 3 | 3 | 3 | 2 | 4                  | 2 | 3 | 2 | 2 | 2 |
| Amman      | 4                  | 3 | 3 | 3 | 3 | 2 | 4                  | 2 | 3 | 2 | 2 | 2 |
| Tripoli    | 4                  | 3 | 3 | 3 | 2 | 2 | 4                  | 2 | 4 | 2 | 2 | 3 |
| Baghdad    | 4                  | 3 | 3 | 3 | 2 | 2 | 4                  | 2 | 4 | 2 | 2 | 3 |
| Damascus   | 4                  | 3 | 3 | 3 | 2 | 2 | 4                  | 2 | 3 | 2 | 2 | 2 |
| Casablanca | 4                  | 3 | 3 | 3 | 2 | 2 | 4                  | 2 | 4 | 2 | 2 | 2 |
| Beirut     | 4                  | 3 | 3 | 3 | 2 | 2 | 4                  | 2 | 3 | 2 | 2 | 2 |
| Tehran     | 4                  | 2 | 3 | 2 | 2 | 2 | 4                  | 2 | 4 | 2 | 2 | 3 |
| Algiers    | 4                  | 2 | 3 | 2 | 2 | 2 | 4                  | 2 | 4 | 2 | 2 | 3 |
| Tunis      | 4                  | 2 | 3 | 2 | 2 | 2 | 4                  | 2 | 4 | 2 | 2 | 3 |
| Ankara     | 4                  | 2 | 3 | 2 | 2 | 2 | 4                  | 2 | 4 | 2 | 2 | 3 |
|            | $\beta = 30^\circ$ |   |   |   |   |   | $\beta = 40^\circ$ |   |   |   |   |   |
| Sanaa      | 4                  | 3 | 3 | 3 | 3 | 2 | 4                  | 3 | 3 | 2 | 2 | 3 |
| Khartoum   | 4                  | 3 | 3 | 3 | 3 | 2 | 4                  | 3 | 3 | 2 | 2 | 3 |
| Muscat     | 4                  | 2 | 3 | 2 | 2 | 3 | 4                  | 2 | 4 | 2 | 2 | 3 |
| Abu-Dhabi  | 4                  | 2 | 3 | 2 | 2 | 2 | 4                  | 2 | 4 | 2 | 2 | 3 |
| Riyadh     | 4                  | 2 | 4 | 2 | 2 | 3 | 4                  | 3 | 4 | 2 | 3 | 3 |
| Doha       | 4                  | 2 | 4 | 2 | 2 | 3 | 4                  | 3 | 4 | 2 | 3 | 3 |
| Manama     | 4                  | 2 | 4 | 2 | 2 | 3 | 4                  | 2 | 4 | 2 | 2 | 3 |
| Kuwait     | 4                  | 2 | 4 | 2 | 2 | 3 | 4                  | 2 | 4 | 2 | 2 | 3 |
| Cairo      | 4                  | 2 | 4 | 2 | 2 | 3 | 4                  | 2 | 4 | 3 | 2 | 4 |
| Jerusalem  | 4                  | 2 | 3 | 2 | 2 | 3 | 4                  | 2 | 4 | 2 | 2 | 4 |
| Amman      | 4                  | 2 | 4 | 2 | 2 | 3 | 4                  | 2 | 4 | 3 | 2 | 4 |
| Tripoli    | 4                  | 2 | 4 | 2 | 3 | 3 | 5                  | 3 | 4 | 3 | 3 | 4 |
| Baghdad    | 4                  | 2 | 4 | 2 | 2 | 3 | 5                  | 3 | 5 | 3 | 2 | 4 |
| Damascus   | 4                  | 2 | 4 | 2 | 2 | 3 | 4                  | 2 | 4 | 3 | 2 | 4 |
| Casablanca | 4                  | 2 | 4 | 2 | 2 | 3 | 4                  | 3 | 4 | 3 | 3 | 4 |
| Beirut     | 4                  | 2 | 4 | 2 | 2 | 3 | 4                  | 2 | 4 | 3 | 2 | 4 |
| Tehran     | 4                  | 2 | 4 | 3 | 2 | 4 | 5                  | 3 | 5 | 3 | 3 | 4 |
| Algiers    | 4                  | 2 | 4 | 3 | 2 | 3 | 5                  | 3 | 4 | 3 | 3 | 4 |
| Tunis      | 4                  | 2 | 4 | 4 | 2 | 3 | 6                  | 3 | 4 | 5 | 3 | 4 |
| Ankara     | 4                  | 2 | 4 | 3 | 2 | 4 | 5                  | 3 | 4 | 3 | 3 | 5 |
|            | $\beta = 50^\circ$ |   |   |   |   |   | $\beta = 60^\circ$ |   |   |   |   |   |
| Sanaa      | 4                  | 3 | 4 | 2 | 3 | 2 | 4                  | 4 | 5 | 3 | 5 | 3 |
| Khartoum   | 4                  | 3 | 4 | 2 | 3 | 2 | 5                  | 5 | 5 | 3 | 5 | 3 |
| Muscat     | 4                  | 3 | 4 | 2 | 3 | 3 | 5                  | 4 | 5 | 3 | 4 | 3 |
| Abu-Dhabi  | 4                  | 3 | 4 | 2 | 3 | 3 | 5                  | 4 | 5 | 3 | 4 | 3 |
| Riyadh     | 5                  | 3 | 5 | 2 | 3 | 3 | 6                  | 4 | 5 | 3 | 5 | 4 |
| Doha       | 5                  | 3 | 5 | 2 | 3 | 4 | 6                  | 4 | 5 | 3 | 5 | 4 |
| Manama     | 5                  | 3 | 4 | 2 | 3 | 3 | 5                  | 4 | 5 | 3 | 4 | 4 |
| Kuwait     | 5                  | 3 | 5 | 3 | 3 | 4 | 5                  | 3 | 5 | 3 | 4 | 4 |
| Cairo      | 5                  | 2 | 5 | 3 | 2 | 4 | 5                  | 3 | 5 | 3 | 3 | 5 |
| Jerusalem  | 5                  | 2 | 4 | 3 | 2 | 4 | 5                  | 3 | 5 | 3 | 3 | 5 |
| Amman      | 5                  | 2 | 4 | 3 | 2 | 4 | 5                  | 3 | 5 | 3 | 3 | 5 |
| Tripoli    | 5                  | 3 | 5 | 3 | 3 | 5 | 6                  | 3 | 5 | 4 | 3 | 5 |
| Baghdad    | 6                  | 3 | 5 | 4 | 3 | 5 | 6                  | 3 | 6 | 4 | 4 | 5 |
| Damascus   | 5                  | 3 | 4 | 3 | 2 | 4 | 5                  | 3 | 5 | 3 | 3 | 5 |
| Casablanca | 5                  | 3 | 5 | 4 | 3 | 4 | 6                  | 3 | 5 | 4 | 3 | 5 |
| Beirut     | 5                  | 2 | 4 | 3 | 2 | 4 | 5                  | 3 | 5 | 3 | 3 | 4 |
| Tehran     | 5                  | 3 | 5 | 4 | 3 | 5 | 6                  | 3 | 6 | 4 | 3 | 5 |
| Algiers    | 5                  | 3 | 5 | 4 | 3 | 5 | 6                  | 3 | 5 | 4 | 3 | 5 |
| Tunis      | 8                  | 4 | 5 | 7 | 5 | 5 | 1                  | 6 | 6 | 9 | 6 | 5 |
| Ankara     | 6                  | 3 | 5 | 4 | 3 | 5 | 6                  | 3 | 6 | 4 | 3 | 6 |
|            | $\beta = 70^\circ$ |   |   |   |   |   | $\beta = 90^\circ$ |   |   |   |   |   |
| Sanaa      | 6                  | 7 | 7 | 4 | 7 | 5 | 9                  | 5 | 7 | 1 | 7 | 1 |
| Khartoum   | 6                  | 7 | 7 | 5 | 7 | 5 | 1                  | 1 | 1 | 1 | 1 | 1 |
| Muscat     | 6                  | 5 | 6 | 3 | 6 | 3 | 9                  | 2 | 2 | 8 | 3 | 7 |

|            |    |   |   |   |   |   |   |   |   |   |   |   |   |
|------------|----|---|---|---|---|---|---|---|---|---|---|---|---|
| Abu-Dhabi  | 6  | 5 | 6 | 3 | 6 | 3 | 9 | 1 | 2 | 1 | 8 | 1 | 7 |
| Riyadh     | 7  | 6 | 6 | 3 | 6 | 3 | 0 | 1 | 1 | 1 | 7 | 1 | 8 |
| Doha       | 7  | 6 | 6 | 4 | 7 | 3 | 0 | 1 | 1 | 1 | 8 | 1 | 8 |
| Manama     | 6  | 5 | 6 | 3 | 6 | 4 | 9 | 2 | 1 | 1 | 7 | 3 | 7 |
| Kuwait     | 6  | 5 | 6 | 3 | 5 | 4 | 9 | 0 | 0 | 0 | 6 | 1 | 5 |
| Cairo      | 6  | 4 | 6 | 4 | 4 | 5 | 9 | 9 | 9 | 9 | 5 | 9 | 5 |
| Jerusalem  | 6  | 4 | 6 | 3 | 4 | 5 | 8 | 8 | 8 | 8 | 5 | 9 | 5 |
| Amman      | 6  | 4 | 6 | 4 | 4 | 5 | 8 | 8 | 8 | 8 | 5 | 9 | 5 |
| Tripoli    | 7  | 4 | 6 | 4 | 4 | 5 | 9 | 8 | 8 | 8 | 4 | 8 | 5 |
| Baghdad    | 7  | 4 | 7 | 5 | 5 | 5 | 1 | 0 | 9 | 9 | 5 | 9 | 5 |
| Damascus   | 6  | 4 | 6 | 4 | 4 | 5 | 8 | 7 | 8 | 4 | 8 | 8 | 5 |
| Casablanca | 6  | 3 | 6 | 4 | 4 | 5 | 8 | 7 | 8 | 5 | 8 | 8 | 5 |
| Beirut     | 6  | 4 | 6 | 4 | 4 | 5 | 8 | 7 | 8 | 4 | 8 | 8 | 5 |
| Tehran     | 7  | 4 | 6 | 5 | 4 | 6 | 9 | 7 | 8 | 5 | 8 | 8 | 5 |
| Algiers    | 6  | 3 | 6 | 5 | 3 | 5 | 8 | 6 | 7 | 5 | 7 | 7 | 5 |
| Tunis      | 11 | 8 | 6 | 0 | 8 | 5 | 2 | 9 | 8 | 0 | 0 | 0 | 6 |
| Ankara     | 7  | 3 | 6 | 5 | 4 | 6 | 8 | 6 | 8 | 6 | 7 | 7 | 7 |

Table 5: The best HBTM for each site corresponding to the tilt angle

| City       | Tilt angle $\beta$ |    |    |    |    |    |    |    |    |
|------------|--------------------|----|----|----|----|----|----|----|----|
|            | 10                 | 20 | 30 | 40 | 50 | 60 | 70 | 80 | 90 |
| Sanaa      | K                  | P  | P  | P  | P  | R  | R  | R  | L  |
| Khartoum   | P                  | P  | R  | R  | P  | R  | R  | R  | L  |
| Muscat     | P                  | P  | R  | R  | R  | R  | R  | R  | P  |
| Abu-Dhabi  | P                  | P  | R  | R  | R  | R  | R  | R  | P  |
| Riyadh     | P                  | P  | R  | R  | R  | R  | R  | R  | R  |
| Doha       | P                  | P  | R  | R  | R  | R  | R  | R  | R  |
| Manama     | P                  | P  | R  | R  | R  | R  | R  | R  | R  |
| Kuwait     | P                  | R  | R  | H  | H  | R  | R  | R  | R  |
| Cairo      | P                  | R  | H  | H  | H  | H  | R  | R  | R  |
| Jerusalem  | P                  | R  | H  | H  | H  | H  | R  | R  | R  |
| Amman      | P                  | R  | H  | H  | H  | H  | R  | R  | R  |
| Tripoli    | P                  | R  | H  | H  | H  | H  | H  | R  | R  |
| Baghdad    | P                  | R  | H  | H  | H  | H  | H  | R  | R  |
| Damascus   | P                  | R  | H  | H  | H  | H  | H  | R  | R  |
| Casablanca | P                  | R  | H  | H  | H  | H  | H  | R  | R  |
| Beirut     | P                  | P  | H  | H  | H  | H  | H  | R  | R  |
| Tehran     | P                  | S  | H  | H  | H  | H  | H  | R  | R  |
| Algiers    | P                  | S  | H  | H  | H  | S  | H  | H  | P  |
| Tunis      | P                  | S  | H  | H  | H  | P  | P  | P  | P  |
| Ankara     | P                  | S  | H  | H  | H  | S  | H  | H  | R  |

It is implicitly shown that the most available HTTMs for MENA region are Hay (32%), HDKR (42%) and Perez (21%), and Skartveit&Olseth (3%) models (Fig.2).

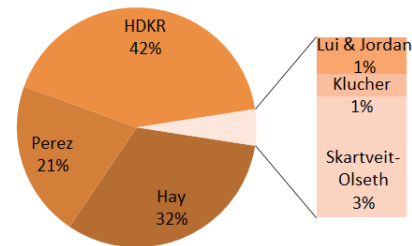


Fig.2: Breakdown of the used HTTMs in MENA region

The  $\beta_{opt}$  for south facing solar collector is also calculating according to the six HTTM for all considered sites and



tabulated in Table 6 combined with the recommended tilt angles from local studies.

Table 6: Optimum tilt angles corresponding to the HTTM

| City       | L  | H  | K  | R  | S  | P  | $\beta_{opt}$ | Ref. |
|------------|----|----|----|----|----|----|---------------|------|
| Sanaa      | 17 | 18 | 17 | 18 | 18 | 19 | 18            | [42] |
| Khartoum   | 17 | 18 | 17 | 18 | 18 | 19 | 19            | [43] |
| Muscat     | 21 | 22 | 22 | 23 | 22 | 24 | 24            | [44] |
| Abu Dhabi  | 21 | 22 | 22 | 23 | 22 | 24 | 22            | [45] |
| Riyadh     | 20 | 22 | 22 | 23 | 22 | 24 | 24            | [46] |
| Doha       | 20 | 21 | 21 | 22 | 21 | 23 | 25            | [47] |
| Manama     | 21 | 22 | 22 | 23 | 22 | 24 | 26            | [48] |
| Kuwait     | 24 | 25 | 25 | 26 | 25 | 26 | 20            | [49] |
| Cairo      | 24 | 26 | 26 | 27 | 26 | 27 | 29            | [50] |
| Jerusalem  | 25 | 27 | 27 | 27 | 27 | 28 | 29            | [51] |
| Amman      | 25 | 27 | 27 | 28 | 27 | 29 | 32            | [52] |
| Tripoli    | 27 | 29 | 28 | 29 | 29 | 30 | 31            | [53] |
| Baghdad    | 26 | 28 | 28 | 29 | 28 | 30 | 30            | [54] |
| Damascus   | 27 | 28 | 28 | 29 | 28 | 29 | 29            | [55] |
| Casablanca | 28 | 30 | 30 | 31 | 30 | 31 | 28            | [56] |
| Beirut     | 26 | 28 | 28 | 28 | 28 | 29 | 28            | [57] |
| Tehran     | 29 | 31 | 30 | 31 | 30 | 32 | 30            | [58] |
| Algiers    | 31 | 33 | 33 | 34 | 33 | 34 | 32            | [59] |
| Tunis      | 29 | 32 | 31 | 37 | 31 | 32 | 35            | [60] |
| Ankara     | 30 | 33 | 32 | 33 | 32 | 34 | 33            | [61] |

It is notic from Table 6 that the Liu&Jordan model is under estimated the recommended optimum tilt angle, while the best model that fits the recommended optimum tilt angles for all sites is the Perez model.

The percentage of reduction in the total annual global solar radiation due to missing the tilt angle is calculated and precented graphically in Fig.3 for the Jursalem city corresponding to all HTTMs.

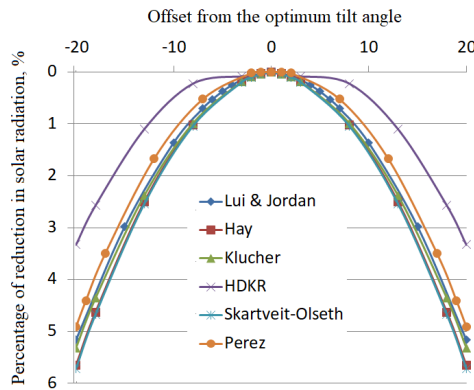


Fig. 3: The effect of offset from the optimum tilt angle on the total annual global tilted solar irradiation

As it tabulated in Table 5, the maximum offset of the optimum tilt angle from all HTTMs is 7° and according to the Fig.3 this will lead to annual reduction in solar energy no more than 1.0% which ranges from 23 (in case of Perez model at  $\beta = 30^\circ$ ) to 21 (in case of Lui&Jordan model at  $\beta = 47^\circ$ ) kWh/m<sup>2</sup>/year

## V. CONCLUSIONS

It has been found that due to the lack of access to meteorological data in many locations around the world, it is convenient for designers or users of solar collectors or photovoltaic (PV) systems to have access to a mathematical model for determining their optimal orientation. This paper

introduces a statistical procedure to figure out the most accuracy transposition model in MENA region without needs to measured data. Also it provided a summary of optimum tilt angles and transposition models that recommended by local researchers for specific locations in MENA region. This study showed that the the most available transposition model for MENA region are Hay (32%), HDKR (42%) and Perez (21%), and it depends strongly on the angle of inclination of the solar collector in addition to the location. The study identified models with deviation rates about 3% for most cities, which is an engineering reasonable percentage, and this encourages to recommend this approach to determine more accurate transposition models for wider regions of the world.. The authors recommend researchers to take care when adopting a transposition model that has been validated at low tilt angles to apply it to high tilt angles and building façades. The reduction in total annual global solar irradiation is not exceeded 1% due to the offset of tilt angle from the optimum angle for all considered transposition models and for all sites.

## REFERENCES

- [1] Y. Nassar, Solar energy engineering- active applications, Sebha - Libya: Sebha university, 2006.
- [2] J. Duffie and W. Beckman, Solar Engineering of Thermal Processes, 4th Edition ed., New York: Wiley, 2013.
- [3] Y. Nassar, "Simulation of solar tracking systems," Energ & Life Journal, vol. 21, pp. 81-90, 2005.
- [4] S. Alsadi, Y. Nassar and K. Amer, "General Polynomial for Optimizing the Tilt Angle of Flat Solar Energy Harvesters Based on ASHRAE Clear Sky Model in Mid and High Latitudes," Energy and Power, vol. 6, no. 2, pp. 29-38, 2016.
- [5] T. Chang, "The Sun's apparent position and the optimal tilt angle of a solar collector in the northern hemisphere," Solar Energy, no. 83, p. 1274-1284, 2009.
- [6] H. Darhmaoui and D. Lahjouji, "Latitude Based Model for Tilt Angle Optimization for Solar Collectors in the Mediterranean Region,," Energy Procedia , no. 42, p. 426 – 435, 2013.
- [7] A. Al-Nuaimi and N. Barrou, "Modeling global, direct, diffuse solar radiation and the optimum tilt angle in some selected Libyan cities," International journal of applied science, vol. 1, no. 1, 2019.
- [8] S. Alsadi and Y. Nassar, "Energy Demand Based Procedure for Tilt Angle Optimization of Solar Collectors in Developing Countries," Fund. Renewable Energy Appl., vol. 7, p. 225, 2017.
- [9] A. Elwani, E. Dekam and K. Agha, "A normalized mathematical model for optimum tilt angles based on the desired solar fraction," International Journal of Recent Development in Engineering and Technology, vol. 8, no. 1, 2019.
- [10] A. Shariah, M. Al-Akhras and I. Al-Omari, "Optimizing the tilt angle of solar collectors," Renewable Energy, vol. 26, p. 587-598, 2020.
- [11] A. Yadav and S. Chandel, "Tilt angle optimization to maximize incident solar radiation: A review," Renewable and Sustainable Energy Reviews, vol. 23, pp. 503-513, 2013.
- [12] A. Hafez, A. Soliman, K. El-Metwally and I. Islam, "Tilt and azimuth angles in solar energy application-A review," renewable an sustainable energy review, vol. 77, pp. 147-168, 2017.
- [13] H. Awad, Y. Nassar, A. Hafez and A. Ali, "Optimal design and economic feasibility of rooftop photovoltaic energy system for assuit University, Egypt," Ain Shams Engineering Journal, vol. 13, no. 3, May 2022.
- [14] H. Muslim, "Solar Tilt Angle Optimization of PV Systems for Different Case Studies," EAI Endorsed Transactions on Energy Web, vol. 7, no. 23, 2019.
- [15] B. Abdullahi, A. S., N. Muhammad, R. Al-Dadah and S. Mahmoud, "Optimum Tilt Angle for Solar Collectors used in Kano, Nigeria," Journal of Advanced Research in Fluid Mechanics and Thermal Sciences, vol. 56, no. 1, pp. 31-42, 2019.
- [16] M. Nfaoui and K. El-Hami, "Optimal tilt angle and orientation for solar photovoltaic arrays: case of Settat city in Morocco," International Journal of Ambient Energy, 2018.
- [17] H. Khorasanizadeh, K. Mohammadi and A. Mostafaiepour, "Establishing a diffuse solar radiation model for determining the

- optimum tilt angle of solar surfaces in Tabass, Iran," *Energy Conversion and Management*, vol. 78, p. 805–814, 2014.
- [18] Y. Nassar and S. Alsadi, "Assessment of solar energy potential in Gaza Strip-Palestine," *Sustainable energy technologies and assessments*, vol. 31, pp. 318–328, 2019.
  - [19] T. Kaddoura, M. Ramli and Y. Al-Turki, "On the estimation of the optimum tilt angle of PV panel in Saudi Arabia," *Renewable and Sustainable Energy Reviews*, vol. 65, p. 626–634, 2016.
  - [20] N. Bailek, K. Bouchouicha, N. Aoun, M. EL-Shimy, B. Jamil and A. Mostafaeipour, "Optimized fixed tilt for incident solar energy maximization on flat surfaces located in the Algerian Big South," *Sustainable Energy Technologies and Assessments*, vol. 28, p. 96–102, 2018.
  - [21] R. Abdallah, A. Juaidi and F. A. S. Abdel-Fattah, "Estimating the Optimum Tilt Angles for South-Facing Surfaces in Palestine," *Energies*, vol. 13, no. 3, p. 623, 2020.
  - [22] M. ŞAHİN, "Determining Optimum Tilt Angles of Photovoltaic Panels by Using Artificial Neural Networks in Turkey," *Technical Gazette*, vol. 26, no. 3, pp. 596–602, 2019.
  - [23] J. Kafka and M. Miller, "The dual angle solar harvest (DASH) method: An alternative method for organizing large solar panel arrays that optimizes incident solar energy in conjunction with land use," *Renewable Energy*, vol. 155, pp. 531–546, 2020.
  - [24] M. Danandeh and S. Mousavi, "Solar irradiance estimation models and optimum tilt angle approaches: A comparative study," *Renewable and Sustainable Energy Reviews*, vol. 92, p. 319–330, 2018.
  - [25] E. Ibrahim, M. Orabi and E. Hasaneen, "Optimum tilt angle for photovoltaic system in desert environment," *Solar energy*, vol. 155, pp. 267–280, 2017.
  - [26] R. Gardashov, M. Eminov, G. Kara, E. Kara, T. Mammadov and X. Huseynova, "The optimum daily direction of solar panels in the highlands, derived by an analytical method," *Renewable and Sustainable Energy Reviews*, vol. 120, 2020.
  - [27] M. Kallioğlu, A. Durmuş, H. Karakaya and A. Yılmaz, "Empirical calculation of the optimal tilt angle for solar collectors in northern hemisphere," *Energy Sources, Part A: Recovery, Utilization, and Environmental*, vol. 42, no. 11, 2019.
  - [28] M. Jacobson, V. Jadhav, "World estimates of PV optimal tilt angles and ratios of sunlight incident upon tilted and tracked PV panels relative to horizontal panels," *Solar energy*, vol. 169, pp. 55–66, 2018.
  - [29] R. Mansour, M. M. Khan, F. Alsulaiman and R. Mansour, "Optimizing the Solar PV Tilt Angle to Maximize the Power Output: A Case Study for Saudi Arabia," *IEEE Access*, vol. 9, pp. 15914–15928, 2021.
  - [30] R. Oprea, M. Istrate, D. Machidon and R. Beniuga, "Determination of Optimum Tilt Angle for Fixed Photovoltaic Modules in Iasi, Romania," 2019 8th International Conference on Modern Power Systems (MPS), pp. 1–6, 21–23 May 2019.
  - [31] S. Alsadi and Y. Nassar, "Correction of the ASHRAE clear-sky model parameters based on solar radiation measurements in the Arabic countries," *International Journal of Renewable Energy Technology Research*, vol. 5, no. 4, pp. 1–16, 2016.
  - [32] S. Alsadi and Y. Nassar, "Estimation of solar irradiance on solar fields: an analytical approach and experimental results," *IEEE transactions on sustainable energy*, vol. 8, no. 4, pp. 1601–1608, 2017.
  - [33] Y. Nassar and S. Alsadi, "View factors of flat solar collectors array in flat, inclined, and step-like solar fields," *Solar energy engineering*, vol. 138, pp. 1–8, December 2016.
  - [34] S. Alsadi and Y. Nassar, "A numerical simulation of a stationary solar field augmented by plan reflectors: Optimum design parameters," *Smart grid and renewable energy*, vol. 8, pp. 221–239, 2017.
  - [35] Y. Nassar, A. Hafez and S. Alsadi, "Multi-Factorial Comparison for 24 Distinct Transposition Models for Inclined Surface Solar Irradiance Computation in the State of Palestine: A Case," *Frontiers Energy Research*, vol. 7, no. 163, 2020.
  - [36] N. Al-Rawahi, Y. Zurigat and N. Al-Azri, "Prediction of hourly solar radiation on horizontal and inclined surfaces for Muscat/Oman," *The Journal of engineering research*, vol. 8, no. 2, pp. 19–31, 2011.
  - [37] K. Samy and A. Shaffie, "Evaluation of transposition models of solar irradiance over Egypt," *Renewable and Sustainable Energy Reviews*, vol. 66, pp. 105–119, 2016.
  - [38] A. Jadallah, M. Dhari and A. Zaid, "Estimation and Simulation of Solar Radiation in Certain Iraqi Governorates," *International Journal of Science and Research*, vol. 3, no. 8, pp. 945–949, 2014.
  - [39] M. Benchirfa, R. Tadili, A. Idrissi, H. Essalhi and A. Mechaqrane, "Development of New Models for the Estimation of Hourly Components of Solar Radiation: Tests, Comparisons, and Application for the Generation of a Solar Database in Morocco," *International Journal of Photoenergy*, pp. 1–16, 2021.
  - [40] A. Noorian, i. Moradi and G. Kamali, "Evaluation of 12 models to estimate hourly diffuse irradiation on inclined surfaces," *Renewable Energy*, vol. 33, no. 6, p. 1406–1412, 2008.
  - [41] A. Mraou, M. K. and B. Benyoucef, "Optimum tilt angle of a photovoltaic system: Case study of Algiers and Ghardaia," in *Proceedings of the fifth international renewable energy congress (IREC)*, Hammamet, Tunisia, 25–27 March 2014.
  - [42] M. Hadwan and A. Alkholidi, "Solar Power Energy Solutions for Yemeni Rural Villages and Desert Communities," *Renewable and Sustainable Energy Reviews*, vol. 57, 2016.
  - [43] S. Abdalla and H. Özcan, "Design and simulation of a 1-GWp solar photovoltaic power station in Sudan," *Clean Energy*, vol. 5, no. 1, p. 57–78, 2021.
  - [44] H. Kazem, M. Chaichan, A. Al-Waeli and K. Sopian, "A novel model and experimental validation of dust impact on grid-connected photovoltaic system performance in Northern Oman," *Solar energy*, vol. 206, pp. 564–578, 2020.
  - [45] F. Jafarkazemi and S. Saadabadi, "Optimum tilt angle and orientation of solar surfaces in Abu Dhabi, UAE," *Renewable energy*, vol. 56, pp. 44–49, 2013.
  - [46] R. Mansour, M. Khan, F. Alsulaiman and R. Mansour, "Optimizing the Solar PV Tilt Angle to Maximize the Power Output: A Case Study for Saudi Arabia," *IEEE Access*, vol. 9, pp. 15914–15928, 2021.
  - [47] F. Touati, M. Al-Hitmi, N. Chowdhury, J. A. Hamad and G. A, "Investigation of solar PV performance under Doha weather using a customized measurement and monitoring system," *Renewable Energy*, vol. 89, pp. 564–577, 2016.
  - [48] C. Georgantopoulou and N. Vasilikos, "Solar Systems Analysis and Estimation for Buildings in Bahrain and GCC Countries," *International Journal of Computing and Digital Systems*, vol. 6, no. 6, pp. 317–329, 2017.
  - [49] M. Adouane, A. Al-QattanBader, B. Alabdulrazzaq and A. Fakhraldeen, "Comparative performance evaluation of different photovoltaic modules technologies under Kuwait harsh climatic conditions," *Energy reports*, vol. 6, pp. 2689–2696, 2020.
  - [50] A. Hegazy, "Estimation of Optimum Tilt Angles for Solar Collector and Gained Energy at Cairo, Egypt," *International Journal of Innovative Science, Engineering & Technology*, vol. 6, no. 5, pp. 249–258, 2019.
  - [51] R. Abdallah, A. Juaidi, S. Abdel-Fattah and F. Agugliaro, "Estimating the Optimum Tilt Angles for South-Facing Surfaces in Palestine," *Energies* 2020, 13, 623, vol. 13, pp. 1–29, 1 February 2020.
  - [52] S. Alrwashdeh, "Determining the Optimum Tilt Solar Angle of a PV Applications at Different Sites in Jordan," *Journal of Engineering and Applied Sciences*, vol. 12, no. 11, pp. 9295–9303, 2017.
  - [53] A. Al-Nuaimi and N. Barrou, "Modeling global, direct, diffuse solar radiation and the optimum tilt angle in some selected Libyan cities," in *The third international conference on basic sciences & their applications*, 2019.
  - [54] A. Morad, A. Al-Sayyab and M. Abdulwahid, "Optimisation of tilted angles of a photovoltaic cell to determine the maximum generated electric power: A case study of some Iraqi cities," *Case Studies in Thermal Engineering*, vol. 12, pp. 484–488, September 2018.
  - [55] S. Soulayman, W. Sabbagh, M. Hamoud and A. Sanduk, "Design and Performance of Two Axes Solar Tracker," *Journal of Solar Energy Research Updates*, vol. 4, pp. 18–28, 2017.
  - [56] M. Nfaoui and K. El-Hami, "Extracting the maximum energy from solar panels," *Eergy reports*, vol. 4, pp. 536–545, November 2018.
  - [57] E. Sassine, "Optimal solar panels positioning for Beirut," in *The 7th International Renewable Energy Congress (IREC)*, Hammamet, Tunisia, 22–24 March 2016.
  - [58] E. Asl-Soleimani, S. Farhangi and M. Zabihi, "The effect of tilt angle, air pollution on performance of photovoltaic systems in Tehran," *Renewable Energy*, vol. 24, no. 3–4, p. 459–468, 2001.
  - [59] A. Mraoui, M. Khelif and B. Benyoucef, "Optimum tilt angle of a photovoltaic system: Case study of Algiers and Ghardaia," in *The fifth international renewable energy congress (IREC)*, Hammamet, Tunisia, 25–27 March 2014.
  - [60] H. Tlijani, A. Aissaoui and R. Younes, "Optimization of tilt angle for solar panel: Case study Tunisia," *Indonesian Journal of Electrical Engineering and Computer Science*, vol. 8, no. 3, pp. 762 – 769, December 2017.
  - [61] K. Bakirci, "General models for optimum tilt angles of solar panels: Turkey case study," *Renewable and Sustainable Energy Reviews*, vol. 16, no. 8, p. 6149–6159, October 2021.